IOP Conf. Series: Journal of Physics: Conf. Series **823** (2017) 012013 doi:10.1088/1742-6596/823/1/012013

Radiation effects of the laser ablative shockwaves on aluminium under atmospheric conditions

S Sai Shiva[1], Ch Leela[1], P Prem Kiran[1], C D Sijoy[2] and S Chaturvedi[2]

[1]Advanced Centre of Research in High Energy Materials (ACRHEM), University of Hyderabad, Hyderabad 500046, India
[2]Computational Analysis Division, Bhabha Atomic Research Centre (BARC), Visakhapatnam, India

E-mail: premkiranuoh@gmail.com

Abstract. Numerical investigation of laser induced shock wave (SW) propagation into bulk aluminium target with and without the effects of electron thermal radiation (ETR and No-ETR) is demonstrated using MULTI-fs 1D-code over intensity range 10^{10} – 10^{11} W/cm^2. The radiation emitting from the plasma is observed to show negligible effects on the SW propagating into aluminium target for low energy (25 mJ) and significant effects at high energy (175 mJ) which was found to be dominant up to 50 ns of time. The observations show that two SW have been launched on to the target surface: one during the pulse duration termed as primary SW (PSW) and the other immediately after the laser pulse termination termed as secondary SW (SSW). The effects of ETR were found dominant on SSW compared to that on PSW for 175 mJ. The PSW and SSW found to coalesce at around 30-40 ns and move as a single SW after these time scales. The resultant pressure after coalesce is higher than the individual ones before coalesce for 175 mJ. The PSW pressures at 25 mJ and 175 mJ were found to be ~1.5 GPa and ~7 GPa, respectively that were launched at 10 ns and 7 ns.

1. Introduction

When a laser beam of sufficiently high intensity is focused on to the target surface, the breakdown of the medium occurs and subsequently formation of plasma takes place due to coupling of laser energy to the target [1]. The plasma then ablates from the target and expands into background gas by absorbing the remaining incoming laser energy until the laser pulse terminates. Due to the ablation, the shock wave (SW) or compression wave (CW) is launched into the target in order to conserve the momentum created by the ablated material [1, 2]. Due to transient laser intensity pulse, the SW launched onto the target also has a transient nature making it a very efficient tool to study the dynamic response of materials. Moreover, with the laser driven shock waves (LDSW) very high pressures over very short durations of time (pulse durations) can be generated unlike the flyer plate impact technique. Due to very high pressures generated at very short times, the impulses will be very high making it efficient technique to generate the equations-of-state [3] of the material. The response of the material to LDSW loadings can give rise to obtain the parameters such as pressure (P), particle (u_p) and shock velocity (U_{sh}), density (ρ) and specific internal energy (E_{sp}) inside the target. The SW pressures launched onto the target depends on various parameters such as target properties, incident laser intensity, wavelength, pulse duration, background gas and also on the radiation emitted from the ablated plasma. The effects of ETR on the ablated plasma and SW expanding into the background

medium for different laser intensities is investigated [4,5] and observed that the radiation plays an important role on the plasma and SW dynamics with the effects becoming significant with increasing laser energy. Many efforts have been made on the LDSW propagating into solid targets [2, 3, 6] and found some of the important aspects [2, 3, 7-9].

In this paper, the numerical simulation of LDSW propagation through bulk aluminum target whose thickness taken to be ~ 2 mm is presented. The intensities ranging between 10^{10} – 10^{11} W/cm^2 were used to launch the SW on to the target surface and the SW dynamics was investigated over the time scales of up to 1000 ns considering with and without electron thermal radiation effects (ETR and No-ETR). The numerical simulations are carried out using modified 1D-radiation hydrodynamic code MULTI-fs [5, 10] for planar, cylindrical and spherical geometries.

2. Simulation methodology

The LDSW in the experiments were launched using the second harmonic of Nd:YAG laser with the excitation wavelength of 532 nm and pulse duration of 7 ns (FWHM). The detailed setup of the experiments presented elsewhere [11, 12]. The simulations have been performed using modified MULTI-fs [5] 1D-RHD code. The laser ablative shock waves (LASW) from Al target propagating into atmospheric air obtained from the simulations are validated [5,11] with the experimental results. Hence the numerical results presented here are the SW propagation into Al target obtained with same input parameters as that in experiments considering the effect of ablation of Al in ambient air. In figure 1, the origin represents the target surface (air-target interface) and the left portion of surface represents the Al target. Similarly the right side represents the background air. The laser is allowed to incident from right to left on to the target surface (origin).

3. Results and Discussion

3.1. Effects of ETR on SW propagating into Al

Figure 1 compares the pressure of shock wave propagating into Al target considering ETR and No-ETR effects for 25 mJ and 175 mJ at 14 and 30 ns, respectively. The origin in figure represents Al-air interface where the laser is incident onto the target surface from right to left.

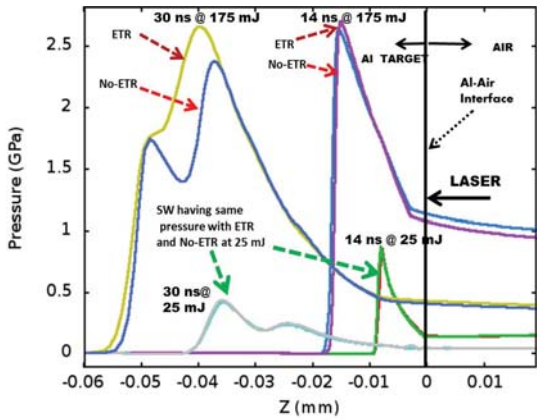

Figure 1. Comparison of shock wave propagating into Al target with ETR and No-ETR effects for 25 mJ and 175 mJ input laser energies at 14 and 30 ns, respectively.

The peak pressures at 25 mJ with ETR and No-ETR found to have same values at both time scales. Whereas with 175 mJ, the pressures are observed to differ slightly at 14 ns, but differ largely at 30 ns. The percentage of laser absorption by the ablated plasma increases with increasing laser energy. Due to increase in the absorption, the electron number density and electron temperatures increases largely within the ablated plasma, also simultaneously the radiation emitting from the plasma increases

due to collisions with the ions. The emitted radiation propagates into ambient air and also into the target. The influence of the ETR effect on the SW propagating in to ambient air validated with experimental data is reported in [5] and observed that the ETR effect become dominant with increasing input laser energy. It is reported [13] that the radiation emitted by the plasma close to the target surface is mostly due to free-free transitions. Since the temperature in the laser affected region within the target increases abruptly, the radiation penetrating into the target increases to over few orders of laser wavelength. This is due to the opacities (Rosseland and Planck) [10] of the material being dependent on temperature and mass density. Since the emissions coming out of the plasma increases in case of 175 mJ, the radiation influence on the SW propagating into targets also becomes prominent at these energies. Hence the pressures were found to have higher values with ETR (~ 2.75 GPa) compared No-ETR (~ 2.3 GPa) at 30 ns. However, the influence of the radiation diminishes quickly at around 50 ns and the SW pressures become similar with ETR and No-ETR.

3.2. Formation and coalescence of the primary and secondary shock wave

In figure 2(a & b) it is clearly visible that two SW emanate inside the Al target. The first one represents the primary shock wave (PSW) that is originated during the initial breakdown of the target within the laser pulse duration. The second one represents the secondary shock wave (SSW) originated immediately after the termination of the laser pulse. During the initial breakdown of the material the plasma expands into the ambient air creating a momentum onto the surface that propagates in the form of PSW into the target. The PSW in case of 25 mJ (figure 2(a)) is observed launching at 10 ns during trailing edge of the laser pulse. Whereas at 175 mJ (figure 2(b)) it occurs at 7 ns during leading edge of the pulse. After the breakdown occurs, the plasma absorbs the remaining laser energy and expands continuously into ambient air until laser pulse terminates. Since the laser interaction time with the ablated plasma is more in case of 175 mJ, the plasma attains very high pressures and temperatures leading to the generation of SSW pressures higher than the PSW. The PSW and SSW pressure at 20 ns with 25 mJ found to be ~ 0.2 GPa and ~ 0.6 GPa, respectively.

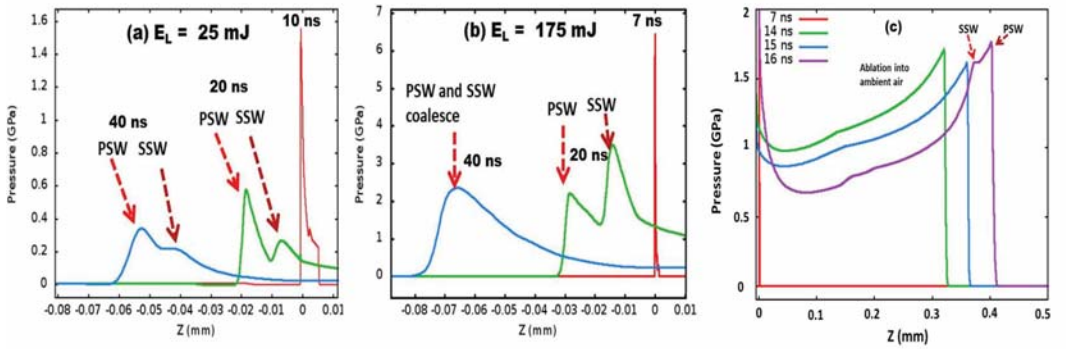

Figure 2. Propagation of the primary and secondary shock wave pressure into Al target at (a) 25 mJ, (b) 175 mJ over the time scales 7 to 40 ns and (c) into ambient air for 175 mJ.

Similarly, with 175 mJ it is found to be ~2 GPa and ~3.5 GPa, respectively. At both the energies it is observed that the two SW (PSW and SSW) coalesce at some point of time during their propagation into target. In the case of 25 mJ, since the strength of SSW is weak compared to PSW, the SW coalesces weakly at around 40 ns. While at 175 mJ, since the SSW strength is more than the PSW the propagation speed will be higher than the PSW. Hence the SSW quickly catches the PSW and coalesces at little early times of around 30 ns. During the coalescence time with 25 mJ, the resultant peak pressure is found have same value as that of PSW before coalescence, whereas with 175 mJ it is found to have higher value than the individual SW before coalescence. Since the two SWs have been generated in to the target correspondingly the SWs will also be generated in the ambient air (shown in

figure 2(c)) in order to conserve the momentum. The SWs propagating in air also coalesce at some point of time where during this time the SW loses its planarity and transfers to the cylindrical nature [5]. The laser ablative shock wave from Al propagating into ambient air is also observed to show an increased velocity at latter time scales [11].

In figure 3 (a & b), the negative particle velocities (u_p) signifies the propagation direction of the SW and particles propagation into Al target. It is obvious from figure 3 (a & b) that, as the pressure increases the particles behind the shock front gain high velocities which is due to high compression of the material particles by the SW. The particle motion follow similar trend as that of the pressure (PSW and SSW) observed in figure 2 (a & b). The particle velocities (u_p) behind the PSW at 25 mJ (figure 3 (a)) were observed to decrease from ~ 0.28 - 0.07 km/s and behind the SSW from ~ 0.06 - 0.05 km/s over 10 – 40 ns and 20-40ns, respectively. Similarly, at 175 mJ (figure 3 (b)) u_p behind PSW it is decreased from ~ 0.85 - 0.4 km/s over 7 – 40 ns and behind SW from ~ 0.6 - 0.4 km/s over 20 – 40 ns.

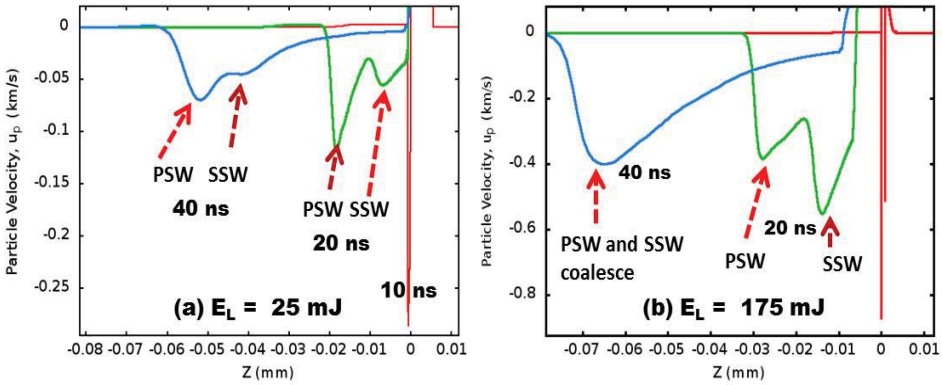

Figure 3. Particle velocities behind the primary and secondary shock wave at (a) 25 mJ and (b) 175 mJ over the time scales 7 to 40 ns.

3.3. Temporal evolution of pressure and particle velocity

In figure 4 (a & b) the temporal evolutions of the pressure and particle velocities is presented for 175 mJ over the time scales of 7 – 1000 ns considering the effects of ETR.

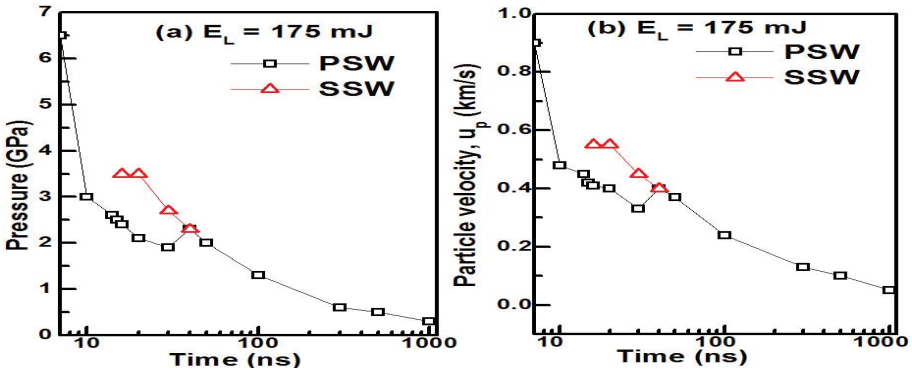

Figure 4. (a) pressure of the SW and (b) particle velocity behind the SW propagating into Al target for the input laser energy of 175 mJ over the time scales of 7 to 40 ns.

The PSW pressure (figure 4 (a)) decay from ~6.5 -1.8 GPa over the time scales 7 – 30 ns and rises to over ~2.4 GPa at 40 ns due to coalescence of PSW and SSW. Similarly, the SSW decays from ~ 3.5 - 2.3 GPa over 16 – 30 ns. The pressure then decreases from ~ 2.3 - 0.25 GPa over 40 – 1000 ns. The

particle velocities (figure 4 (b)) behind the PSW decay from ~ 0.9 - 0.3 km/s over the time scales 7 – 30 ns and rises to over ~ 0.4 km/s at 40 ns due to coalescence of PSW and SSW. Similarly, the particle velocities behind SSW decay from ~0.58 - 0.4 km/s over 16 – 30 ns. Finally, the particle velocities decrease from ~ 0.4 - 0.1 km/s over 40 – 1000 ns.

3.4. P - u_p Hugoniot

Figure 5 corresponds to the P - u_p Hugoniot curve of the Al target obtained for two laser energies 25 mJ and 175 mJ, respectively. As observed from figure that as the shock pressure increases the particle velocities also increases linearly. The maximum particle velocity at 1 GPa observed to be ~ 0.18 km/s (at 25 mJ) similarly, at 6.5 GPA observed to be ~ 0.9 km/s. The highest SW velocity (U_{sh}) achieved with 25 mJ and 175 mJ found to be ~2.0 km/s and 2.6 km/s. So the maximum particle velocities attained at pressures 1 and 6.5 GPa are very small compared to the maximum shock speeds achieved.

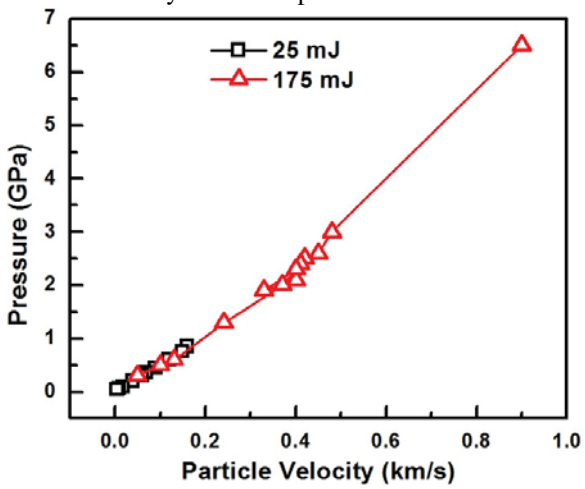

Figure 5. P-u Hugoniot curve for the input laser energies of (a) 25 mJ and (b) 175 mJ.

4. Conclusion

Numerical simulations performed with 1D-RHD code show that the laser driven shock waves (LDSW) propagating into Al target are dependent on the incident laser energy. At low input laser energy (25 mJ) the ETR effects on laser driven shock waves (LDSW) propagating into Al target show negligible influence on the pressure and particle velocity evolution. So the SW pressure, particle velocity behind SW was found to have similar values with ETR and No-ETR effects. While at high input laser energy (175 mJ) the radiation found to play a significant role on the SW propagation. The shockwave pressure increased with increasing laser energy. One important aspect observed from the simulations is that two SW (PSW and SSW) emanating into the target. The first SW was launched during the laser pulse interaction and the second SW immediately after termination of the laser pulse. The PSW pressure in case of low laser energy is observed to have higher pressure than the SSW pressure whereas at high laser energy the SSW is observed to have higher shock pressure. The role of ETR effects on PSW is found to be small compared to that of the SSW at 175 mJ which confirms that the radiation emitting from ablated plasma is small during the laser pulse interaction process and becomes significant after the laser pulse termination due to expansion and cooling of the ablated plasma. The ETR effects are found to play a significant role up to 50 ns time scales and later on show negligible effects on the SW propagation. The two shock waves were observed to coalesce at around 30 – 40 ns and finally propagate as single shock wave. The two SWs observed to be generated in ambient air and found to coalesce at around 50 ns where during this time SW was observed to transit from planar to cylindrical nature. This was observed to lead to laser ablative shock propagating with varying velocities at latter time scales [11]. During the coalescence time the resultant SW is found to have

higher pressure than the individual one before coalesce. The P - u_p Hugoniot of Al target is presented from 1- 6.5 GPa SW pressure.

Acknowledgement
Authors from ACRHEM (S Sai Shiva, Ch Leela and P Prem Kiran) thank DRDO for Grants-in-Aid funding.

References
[1] Radziemski L J, Cremers D A 1989, *Laser-induced plasmas and applications* (New York:Marcel Dekker Inc)
[2] Benuzzi-Mounaix A, Koenig M, Ravasio A et al. 2006 *Plasma Phys. Control. Fusion* **48** B347
[3] Remington B A, Drake R P, Takabe H, Arnett D 2000 ,*Phys. Plasmas* **7** 1641
[4] Laville S, Vidal F, Johnston T W, Chaker M, Le Drogoff B, Barthélemy O, Margot J, Sabsabi M 2004 ,*Phys. Plasmas* **11** 2182
[5] Sai Shiva S, Leela C, Prem Kiran P, Sijoy C D, Chaturvedi S 2016 ,*Phys. Plasmas* **23** 053107
[6] Batani D, Stabile H, Ravasio A, Lucchini G, Strati F, Desai T, Ullschmied J, Krousky E, Skala J, Juha L, Kralikova B, Pfeifer M, Kadlec C, Mocek T, Präg A, Nishimura H, Ochi Y 2003 ,*Phys. Rev. E* **68** 067403
[7] Luo S N, Swift D C, Tierney IV, Paislet D L, Kyrala G A, Johnson R P, Hauer A A, Tschauner O and Asimow P D, 2004 *High Pressure Res.* **24** 409
[8] Thibaut de R, Didier L, Andre D and Emilien L 2014 ,*Metals* **4** 490
[9] Atzeni S, Ribeyre X, Schurtz G, Schmitt A J, Canaud B, Betti R and Perkins L J 2014 , *Nucl. Fusion* **54** 054008
[10] Ramis R, Eidmann K, Meyer-ter-Vehn J, Hüller S 2012, *Comput. Phys. Commun.* **183** 637
[11] Leela C, spatio temporal imaging of laser induced shock waves and plasma plume from ambient air, metals, periodic structured surfaces and sub-micron sized compacted powders 2014 Ph. D. thesis University of Hyderabad India
[12] Leela C, Venkateshwarlu P, Singh R V, Verma P, Kiran P P 2014 ,*Opt. Express* **22** A268
[13] Rezaei F, Tavassoli S H 2013 ,*Phys. Plasmas* **20** 013301